

# Propagation of massless particles around a BTZ-ModMax black hole

**Shubham Kala**

The Institute of Mathematical Sciences  
C.I.T Campus, Taramani, Chennai-600113, Tamil Nadu, India

E-mail: [shubhamkala871@gmail.com](mailto:shubhamkala871@gmail.com)

**Abstract.** We investigate the deflection of light around a BTZ-ModMax black hole, focusing on the influence of the ModMax parameter and the cosmological constant. The trajectories of massless particles are explored through an analysis of null geodesics, providing deeper insights into the gravitational lensing effects in this modified black hole geometry. Using the Gauss-Bonnet theorem, we derive the deflection angle of light and provide a detailed examination of how the ModMax parameter and the cosmological constant impact the bending of light. Furthermore, we compare the deflection results obtained for the BTZ-ModMax black hole with those of the charged and static BTZ black hole solution, highlighting key differences and insights into the role of nonlinear electrodynamics in the gravitational lensing phenomena. This study provides valuable insights into the deflection of light in modified black hole solutions within the framework of lower-dimensional geometry, highlighting the complex relationship between nonlinear dynamics and spacetime curvature.

**Keywords:** Black holes, nonlinear electrodynamics, null geodesics, stability, light deflection

---

## Contents

<b>1</b>	<b>Introduction</b>	<b>1</b>
<b>2</b>	<b>BTZ-ModMax BH Spacetime</b>	<b>3</b>
2.1	Field equation for ModMax NLED theory	3
2.2	Horizon Structure	4
<b>3</b>	<b>Null Geodesics</b>	<b>5</b>
3.1	Geodesic equations and Effective Potential	5
3.2	Photon Sphere and possible types of trajectories	6
3.3	Stability of Null Geodesics	7
3.4	Gaussian Optical Curvature	9
<b>4</b>	<b>Deflection of Light</b>	<b>10</b>
<b>5</b>	<b>Summary and conclusions</b>	<b>13</b>

---

## 1 Introduction

Nonlinear electrodynamics (NLED) theories are generalizations of Maxwell’s theory that address phenomena beyond its scope, such as the self-interaction of virtual electron-positron pairs and the elimination of spacetime singularities in black holes (BHs) [1–3]. These theories also influence gravitational redshift around strongly magnetized compact objects and eliminate the cosmological singularity associated with the Big Bang [4–8]. Examples of NLED theories include Born-Infeld (BI) [9], Euler-Heisenberg (EH) [1], and Power-Law (PL) [10, 11]. Each theory has distinct properties, such as electromagnetic duality, conformal invariance, and the resolution of self-energy divergences in point particles. Recently, the Modified-Maxwell (ModMax) NLED theory was introduced [12], distinguished by the dimensionless parameter  $\gamma$ , which recovers Maxwell’s theory for  $\gamma = 0$  [13]. Coupling ModMax electrodynamics with gravity has led to various BH solutions, expanding our understanding of spacetime and field interactions [14–16]. The first-ever BH solution in (2+1)-dimensional gravity within the framework of General Relativity (GR) was proposed by Bañados, Teitelboim, and Zanelli in 1992, and it is widely recognized as the BTZ BH [17]. This BH solution features a negative cosmological constant and exists in lower dimensions, it has opened a new and exciting field of study in theoretical physics, offering unique insights into lower dimensional gravity. The BTZ BH, unlike (3+1)-dimensional solutions such as Schwarzschild and Kerr, is asymptotically anti-de Sitter and has no curvature singularity at the origin [18]. However, it retains key features like an event horizon, Hawking temperature, and well-defined thermodynamic properties, offering valuable insights into lower-dimensional gravity. [19]. Then, the study of gravity in three-dimensional spacetime absorbed a lot of attentions due to different aspects of their physics properties. In this regard, different three-dimensional BHs have been obtained in Einstein’s gravity and also modified theories of gravity which are coupled with linear and nonlinear matters [20–27]. More recentaly, an analytic BTZ BH solution is obtained by coupling Einstein’s gravity with the ModMax NLED field followed by

detailed thermal properties [28]. Geodesics are fundamental to the study of spacetime geometry, as they describe the trajectories of test particles and light rays in a curved spacetime [29]. They provide critical information about the causal structure of spacetime, the nature of gravitational interactions, and the response of the spacetime to the presence of mass and energy, serving as a key tool for understanding the dynamics of relativistic systems. In the context of a  $(2 + 1)$ -dimensional BH, geodesics describe the trajectories followed by massless and massive particles under the influence of the BH's gravitational field [30]. The detailed study of geodesics structure provide essential insights into the behavior of light and matter around the BH, revealing properties like the deflection of light, event horizon structure, and thermodynamic characteristics. Understanding geodesics in such lower-dimensional spacetimes helps to explore fundamental aspects of gravity and spacetime curvature in reduced dimensions. The analysis of geodesics in lower-dimensional frameworks, as explored by previous authors, is referenced herein [31–36]. Over the past few decades, gravitational lensing (GL) has been extensively studied due to its profound implications in astrophysics. The gravitational deflection of light was first quantitatively analyzed by Soldner in 1801 using Newtonian mechanics [37]. In 1959, Darwin extended this analysis and obtained the deflection angle of light in strong-field regime using the Schwarzschild metric [38]. Further studies explored the deflection angle and the formation of images due to the Schwarzschild BH, with expressions involving elliptic integrals of the first kind. Virbhadra and Ellis introduced a lens equation for strong GL by a Schwarzschild BH and proposed a method to compute the bending angle [39]. Iyer et al., formulated an analytical perturbative approach to calculate the bending angle of light rays, lensed by a Schwarzschild BH [40]. W. Rindler and M. Ishak [41] investigated the influence of the cosmological constant on the deflection of light, providing critical insights into its role in gravitational lensing phenomena. Gibbons and Werner introduced a straightforward yet elegant method for studying GL, utilizing the Gauss-Bonnet theorem (GBT) to derive the deflection angle through the Gaussian optical curvature of spherically symmetric spacetime [42]. Bozza further advanced the understanding of strong lensing by considering a spherically symmetric BH, where an infinite series of higher-order images are formed, later extending the framework to include rotating BHs [43]. Furthermore, Ishihara et al. [44], extended the Gibbons-Werner method to spacetimes with rotating BHs, using the optical geometry approach. Their method provided a more intuitive framework for understanding the deflection of light in curved spacetime, highlighting the connection between geometry and the bending of light in gravitational fields. Ono et al. [45], studied the effects of finite distance on the gravitational deflection angle of light. Fathi et al. [46], investigated the deflection angle of massless particles in a static BTZ BH background within the framework of scale-dependent gravity. Additionally, Kala et al. [47], derived an exact expression for the bending angle of light around a rotating BTZ BH. Furthermore, Upadhyay et al. [48], analyzed the weak deflection angle of a charged massive BTZ BH. Notably, the study of light propagation in the vicinity of ModMax BH in  $(3+1)$  dimensional geometry reported by Herrera et.al [49]. Numerous other studies have also explored the deflection of massless particles in lower-dimensional spacetimes, with relevant references provided herein [50–53]. In this paper, we aim to investigate various aspects of light propagation around a ModMax BH, including null geodesics, possible trajectories, the stability of null geodesics, Gaussian optical curvature, and the deflection angle of light. The outline of this manuscript is as follows: In Section 2, we examine the BTZ-ModMax black hole spacetime, focusing on its horizon structure in Subsection 2.2. Section 3 discusses null geodesics, including their stability (Subsection 3.3) and the Gaussian optical curvature (Subsection 3.4). In Section 4,

we investigate the deflection of light around this spacetime. Finally, Section 5 summarizes the key findings and conclusions of this work.

## 2 BTZ-ModMax BH Spacetime

### 2.1 Field equation for ModMax NLED theory

The action describing Einstein's theory of gravitation coupled with ModMax NLED and the cosmological constant in a three-dimensional spacetime is given by [12],

$$I = \frac{1}{16\pi} \int_{\partial M} d^3x \sqrt{-g} [R - 2\Lambda - 4L], \quad (2.1)$$

where  $R$  is the Ricci scalar, and  $\Lambda$  is the cosmological constant. The parameter  $g = \det(g_{\mu\nu})$ , denotes the determinant of the metric tensor  $g_{\mu\nu}$  and  $L$  represents the ModMax Lagrangian [13]. We assume that the ModMax Lagrangian in three-dimensional spacetime takes a form analogous to the ModMax Lagrangian in four-dimensional spacetime, expressed in by the following relation,

$$L = X \cosh \gamma - \sqrt{X^2 + Y^2} \sinh \gamma, \quad (2.2)$$

where,  $\gamma$  is a dimensionless parameter known as the ModMax parameter. In the ModMax Lagrangian,  $X$  and  $Y$ , respectively, are a true scalar and a pseudoscalar. They are defined as,

$$X = \frac{F}{4}, \quad (2.3)$$

$$Y = \frac{Fe}{4} \quad (2.4)$$

where  $F = F_{\mu\nu}F^{\mu\nu}$  is the Maxwell invariant and  $F_{\mu\nu}$  is called the electromagnetic tensor field.  $F_{\mu\nu}$  can be calculated as given,

$$F_{\mu\nu} = \partial_\mu A_\nu - \partial_\nu A_\mu, \quad (2.5)$$

where,  $A_\mu$  is the gauge potential. In addition,  $Fe = F_{\mu\nu}F^{\mu\nu}$ , and  $Fe_{\mu\nu} = \frac{1}{2}\epsilon_{\rho\lambda\mu\nu}F^{\rho\lambda}$ . It is notable that the ModMax Lagrangian reduces to the linear Maxwell theory, i.e.,  $L = \frac{F}{4}$ , when  $\gamma = 0$ . The BTZ BH solution within framework of the ModMax theory is therefore given by [28],

$$ds^2 = -\psi(r) dt^2 + \frac{dr^2}{\psi(r)} + r^2 d\phi^2, \quad (2.6)$$

where the metric function is defines as,

$$\psi(r) = -m_0 - \Lambda r^2 - 2q^2 e^{-\gamma} \ln\left(\frac{r}{r_0}\right). \quad (2.7)$$

Here,  $m_0$  is an integral constant which is related to the total mass of BH.  $r_0$  is an arbitrary length parameter and  $q$  represents the charge of BH.  $\Lambda$  is the cosmological constant already defined earlier. Throughout the manuscript, we have considered its negative value.  $\gamma$  is a ModMax parameter and in absence of this parameter the metric turns into BTZ BH in Einstein- $\Lambda$ -Maxwell theory.

## 2.2 Horizon Structure

We analyze the behavior of the metric function as a function of radial distance to study the nature of the horizons. By fixing the charge and the cosmological constant parameters, we observe that for larger values of the ModMax parameter, two horizons are present: an inner horizon and an outer (BH) horizon. Additionally, when the ModMax parameter is held constant and the cosmological constant is varied, we find that decreasing the value of the cosmological constant results in the existence of only a single horizon. However, two horizons are observed within a specific range of parameter values. As a result, small charged AdS BTZ BHs with large values of the ModMax parameter and mass have two roots, which are inner root and event horizon, respectively.

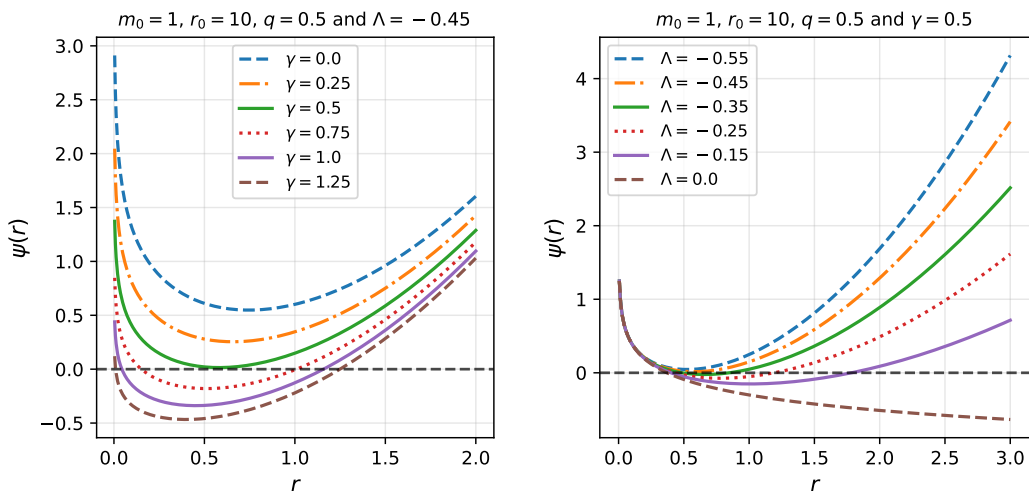


**Figure 1.** The variation of metric function with radial distance for different values of ModMax and Cosomological constant parameter.

The analytical solution of the BH horizon can be obtained using the method outlined in [54]. Accordingly, the horizons radii of the BH are determined as follows,

$$r_+ = r_0 \exp \left( -\frac{1}{2} \left[ W \left( \frac{r_0^2 e^{\left( -\frac{m_0}{q^2 e^{-\gamma}} \right)}}{q^2} \right) + \frac{m_0}{q^2 e^{-\gamma}} \right] \right), \quad (2.8)$$

$$r_- = r_0 \exp \left( -\frac{1}{2} \left[ W \left( -1, \frac{r_0^2 e^{\left( -\frac{m_0}{q^2 e^{-\gamma}} \right)}}{q^2} \right) + \frac{m_0}{q^2 e^{-\gamma}} \right] \right), \quad (2.9)$$

where,  $W(x)$  denotes the principal branch of the Lambert  $W$  function and  $W(-1, x)$  the branch with  $W(-1, x) \leq -1$ . For a comprehensive and detailed discussion on the Lambert  $W$  function, readers are referred to [55].  $r_+$  and  $r_-$  represent the outer and inner horizons of BH respectively. The only physically acceptable solution of Eqs. 2.8 and 2.9 is,

$$r_+ > 0 \quad \text{or} \quad r_- > 0 \quad \text{so} \quad m_0 \geq q^2 \left( \ln \left( -\frac{r_0^2}{e^{-\gamma} q^2} \right) + 1 \right) \quad \text{for} \quad q < 0.$$

From the above expression, it is evident that the BH horizon is influenced by various parameters, such as  $\gamma$ ,  $q$ , and other BH characteristics. The effect of these parameters on the horizon is clearly illustrated in the photon trajectories, where the BH horizon is represented by a black solid sphere.

### 3 Null Geodesics

#### 3.1 Geodesic equations and Effective Potential

Geodesic equations can be obtained using Lagrangian equation corresponding to a given spacetime is below,

$$L = g_{\mu\nu} \frac{dx^\mu}{d\lambda} \frac{dx^\nu}{d\lambda} = -\epsilon = -\psi(r) \left( \frac{dt}{d\lambda} \right)^2 + \frac{1}{\psi(r)} \left( \frac{dr}{d\lambda} \right)^2 + r^2 \left( \frac{d\phi}{d\lambda} \right)^2, \quad (3.1)$$

where  $\epsilon$  takes the values 1 and 0 for massive and massless particles, respectively, and  $\lambda$  is the affine parameter for massless particles and the proper time for massive particles. Since we are working in static and spherically symmetric spacetimes, we can immediately obtain two conserved quantities, energy and angular momentum, as:

$$E = g_{tt} \frac{dt}{d\lambda} = -\psi(r) \frac{dt}{d\lambda}, \quad L = g_{\phi\phi} \frac{d\phi}{d\lambda} = r^2 \frac{d\phi}{d\lambda}. \quad (3.2)$$

From this, we then find the following geodesic equations,

$$\left( \frac{dr}{d\lambda} \right)^2 = E^2 - \psi(r) \left( \frac{L^2}{r^2} + \epsilon \right), \quad (3.3)$$

The effective potential corresponding to null geodesics then given by,

$$V_{\text{eff}}(r) = \left\{ -m_0 - \Lambda r^2 - 2q^2 e^{-\gamma} \ln \left( \frac{r}{r_0} \right) \right\} \frac{L^2}{r^2}. \quad (3.4)$$

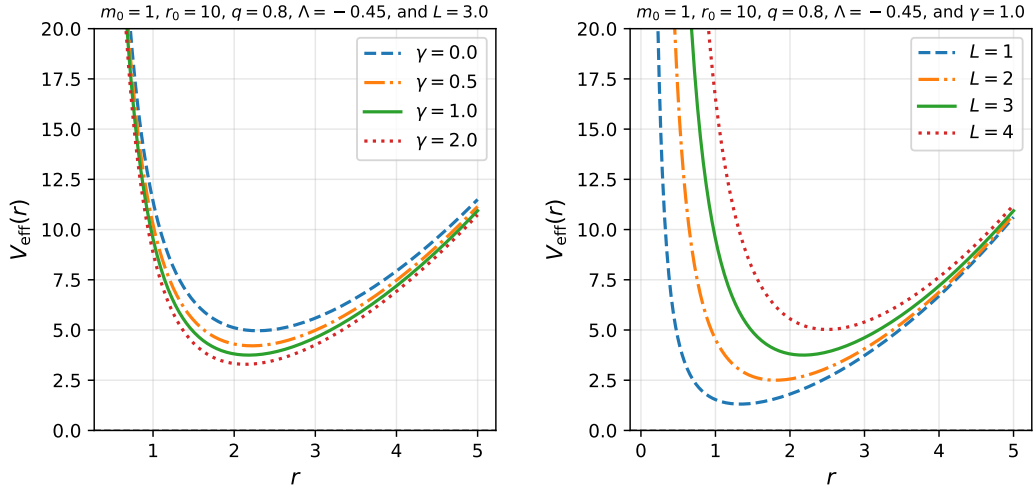


**Figure 2.** The variation of effective potential with radial distance for different values of ModMax parameter and angular momentum of massless particles.

The variation of the effective potential with the radial distance for different ModMax parameters and angular momentum values of massless particles is shown in Fig. 2. It is evident that the effective potential has a single minimum, suggesting the possibility of stable photon orbits around the BH. Notably, as the ModMax parameter increases, the effective potential decreases, indicating a reduction in the electrostatic repulsion between the BH and photons. This weakening of the repulsive interaction allows more particles to escape from the BH's gravitational field. Furthermore, the effective potential reaches its maximum for the highest values of angular momentum, as the increased centrifugal force pushes the particles outward, preventing them from falling into the BH.

### 3.2 Photon Sphere and possible types of trajectories

The radii of the photon sphere can be determined using the condition for circular null geodesics, which requires  $\dot{r} = 0 \Rightarrow V_{\text{eff}} = 0$ ,  $V'_{\text{eff}}(r) = 0$ . By solving these conditions analytically, the radius of the photon sphere is obtained, and the resulting expression is given as,

$$r_{ph} = r_0 \exp \left\{ \frac{1}{2} \left( 1 - \frac{m_0}{q^2 e^{-\gamma}} \right) \right\}. \quad (3.5)$$

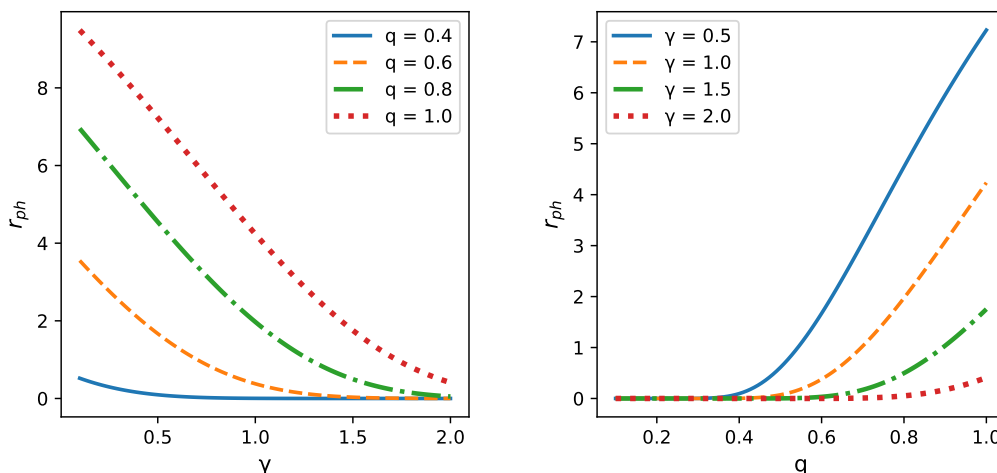


**Figure 3.** The graph shows the radii of photon sphere for the ModMax BTZ BH as a function of the ModMax parameter (left panel) and charge parameter (right panel). Here, we consider  $m_0 = 1$  and  $r_0 = 10$ .

The variation in the radii of the photon sphere for different ModMax parameters and charge values is illustrated in Fig. 3. It is evident that the radius of the photon sphere decreases with increasing  $\gamma$ , while it increases as the charge parameter grows. Additionally, we observe that for very small values of the charge parameter, the photon sphere does not exist for any value of  $\gamma$ . Notably, the photon sphere is independent of the cosmological constant.

In order to analyze the trajectories of the geodesic equation we obtain the equation of motion as,

$$\left( \frac{dr}{d\phi} \right)^2 = \frac{r^4}{L^2} \left\{ E^2 - \left( -m_0 - \Lambda r^2 - 2q^2 e^{-\gamma} \ln \left( \frac{r}{r_0} \right) \right) \frac{L^2}{r^2} \right\}, \quad (3.6)$$

and, with the change of variable  $u = 1/r$ ,

$$\left(\frac{du}{d\phi}\right)^2 = \left\{ \frac{1}{b^2} - \left( -m_0 - \Lambda \frac{1}{u^2} - 2q^2 e^{-\gamma} \ln\left(\frac{1}{ur_0}\right) \right) \frac{1}{u^2} \right\}. \quad (3.7)$$

where,  $b = L/E$  the impact parameter. We numerically solved the Eq. 3.7 and depicted the possible types of trajectories in Fig. 4. Based on the values of angular momentum, energy, and black hole parameters, two distinct types of orbit can be identified. The first type is bound orbits, where massless particles fall into the BH horizon and cannot escape. The second type is flyby orbits, where particles originating from infinity approach the black hole but ultimately escape back to infinity. We identified two distinct types of flyby orbits: one is the simple flyby orbit, where the particle approaches the BH and escapes to infinity within the same asymptotic region, and the other is the two-world flyby orbit, where the particle transitions from one asymptotic region to another. The existence of two-world flyby orbits is justified by the spacetime structure of the BH, particularly in cases where the geometry includes multiple asymptotic regions, such as in extended or maximally extended spacetimes, allowing particles to traverse between these regions without being captured by the BH. A detailed analysis of the definitions and characteristics of these orbits can be found in [56].

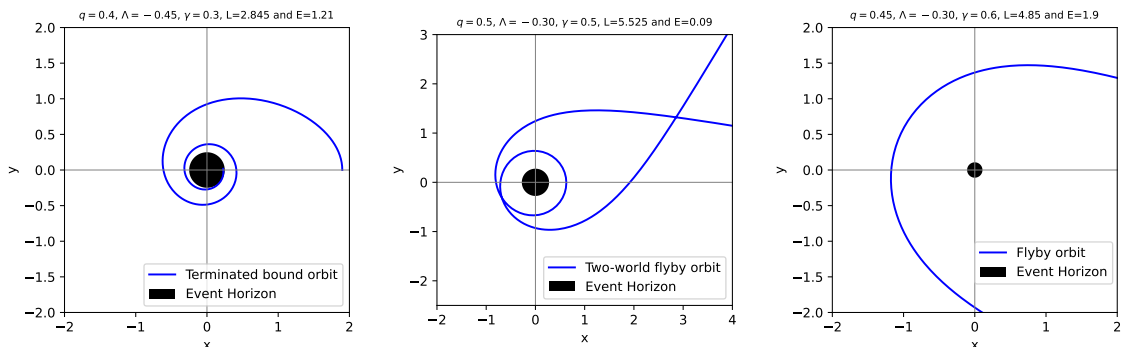


**Figure 4.** The figure shows three types of photon trajectories around a BH: terminated bound orbit (fall into the singularity), two-world flyby orbit (traverses near the BH and then escape to infinity) and flyby orbit (escape to infinity).

### 3.3 Stability of Null Geodesics

In this subsection, we analyze the stability of null circular geodesics, we construct a dynamical system and analyze its phase space structure in the  $(r, \dot{r})$  plane [57]. The study of the behavior of small perturbations around the circular geodesics enables us to determine whether the orbits are stable or unstable under radial perturbations. The condition  $\dot{r} = 0$  in null geodesics, implies that the radial velocity vanishes, leading to a reduction of the phase space dynamics to a two-dimensional subspace characterized by the variables  $r$  and its conjugate momentum. Analyzing the phase flow dynamics in the  $(r, \dot{r})$  plane allows us to identify the critical point associated with the photon orbit radius  $(r_c, 0)$ . To advance this analysis, we differentiate Eq. 3.3 with  $\epsilon = 0$ , eliminating  $\dot{r}$  to derive the following expression,

$$\ddot{r} = -\frac{dV_{\text{eff}}}{dr}. \quad (3.8)$$



Now we consider the coordinates  $x_1 = \dot{r}$  and  $x_2 = \dot{x}_1$ , leading to the differential equations corresponding to these coordinates, which are given by,

$$\begin{aligned} x_1 &= \dot{r}, \\ x_2 &= -\frac{dV_{\text{eff}}}{dr}. \end{aligned} \quad (3.9)$$

The Jacobian matrix  $J$  corresponding to the sets of differential Eq. 3.9 is given by [58],

$$J = \begin{pmatrix} 0 & 1 \\ -V''_{\text{eff}}(r) & 0 \end{pmatrix}, \quad (3.10)$$

where,  $V''_{\text{eff}}(r)$  denotes the second derivative of the effective potential with respect to  $r$ . The secular equation  $|J - \lambda I| = 0$  yields the eigenvalue squared as,

$$\lambda_L^2 = -V''_{\text{eff}}(r). \quad (3.11)$$

Here,  $\lambda_L$  is known as the Lyapunov exponent. It measure the average rate at which nearby trajectories converge or diverge in the phase space.  $\lambda_L^2 > 0$  indicates a divergence between nearby trajectories, i.e., the behavior of the system exhibits both stable and unstable directions (saddle critical points). Conversely, the condition  $\lambda_L^2 < 0$  indicates a convergence between nearby trajectories, i.e., critical point represents a stable center.

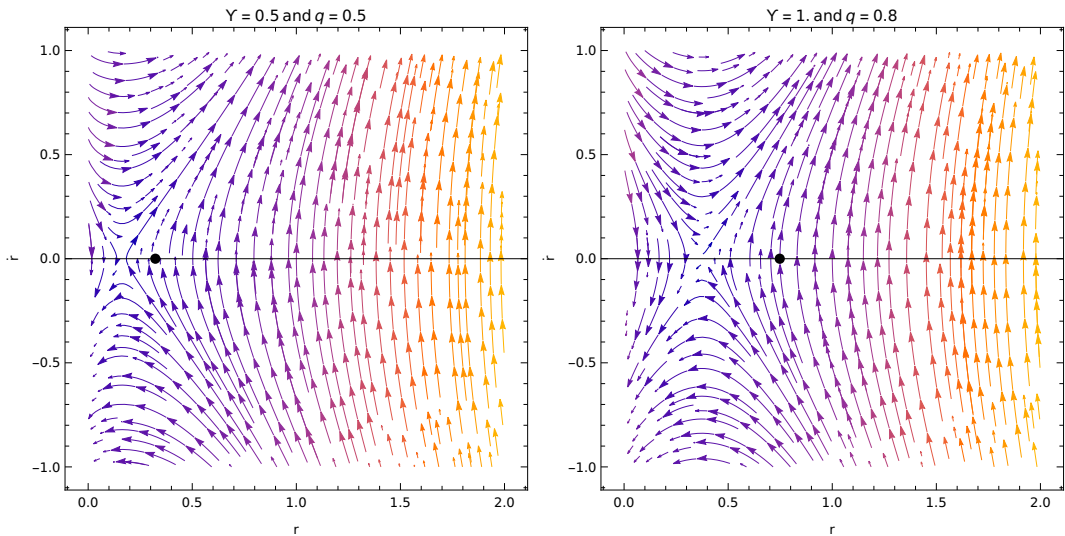


**Figure 5.** The graph shows the phase portrait  $r$  vs  $\dot{r}$  of the null geodesics for different combination of the parameter  $\gamma$  and  $Q$ .

The phase portraits in Fig. 5 illustrate the behavior of null geodesics in the  $r - \dot{r}$  plane for different values of the parameters  $\gamma$  and  $q$ . In the left plot  $\gamma = 0.5$ ,  $q = 0.5$ , the trajectories indicate a relatively stable configuration, with orbits converging towards the critical point where  $\dot{r} = 0$ . In the right plot  $\gamma = 1.0$ ,  $q = 0.8$ , the flow becomes more dynamic, with trajectories diverging more prominently from the critical point. This demonstrates that higher values of  $\gamma$  and  $q$  increase the influence of the BH parameters, altering the stability and behavior of the photon orbits.

### 3.4 Gaussian Optical Curvature

In this subsection we now focus on null geodesics deflected by this BH to analyze the gaussian optical curvature using the optical metric. It is well-established that light follows null geodesics, which are characterized by the condition (i.e.,  $ds^2 = 0$ ). This null condition is fundamental in defining the optical metric, which effectively captures the geometry traced by light as it propagates through a curved spacetime. In this context, the optical metric provides an approximation of the Riemannian geometry experienced by photons, facilitating the study of phenomena such as GL and light deflection. Incorporating the condition of null geodesics, the associated optical metric is given by [44],

$$dt^2 = \bar{g}_{ij} dx^i dx^j = d\tilde{r}^2 + \psi(\tilde{r})^2 d\phi^2, \quad (3.12)$$

where

$$d\tilde{r} = \frac{dr}{\sqrt{-m_0 - \Lambda r^2 - 2q^2 e^{-\gamma} \ln\left(\frac{r}{r_0}\right)}}, \quad (3.13)$$

$$\psi(\tilde{r}) = \frac{r}{\sqrt{-m_0 - \Lambda r^2 - 2q^2 e^{-\gamma} \ln\left(\frac{r}{r_0}\right)}}. \quad (3.14)$$

The equatorial plane within the optical metric represents a surface of revolution. The Christoffel symbols corresponding to the metric in Equation 3.12, which are non-zero, are determined as follows,

$$\tilde{\Gamma}_{\phi\phi}^r = \frac{r(r\psi'(\tilde{r}) - 2\psi(\tilde{r}))}{2}, \quad (3.15)$$

$$\tilde{\Gamma}_{r\phi}^\phi = \frac{2\psi(\tilde{r}) - r\psi'(\tilde{r})}{2}, \quad (3.16)$$

$$\tilde{\Gamma}_{rr}^r = -\frac{\psi'(\tilde{r})}{\psi(\tilde{r})}. \quad (3.17)$$

Here, the prime indicates differentiation with respect to  $r$ . Using the Christoffel symbols derived above, the only non-zero components of the Riemann tensor that contribute to the optical curvature are as follows,

$$\tilde{R}_{\phi r\phi}^r = -\kappa\psi^2(\tilde{r}). \quad (3.18)$$

Thus, the Gaussian optical curvature  $\mathcal{K}$  can be expressed in term of Ricci scalar through the following relation,

$$\mathcal{K} = \frac{R}{2} = -\frac{1}{\psi(\tilde{r})} \left[ \frac{dr}{d\tilde{r}} \frac{d}{dr} \left( \frac{dr}{d\tilde{r}} \right) \frac{d\psi}{dr} + \frac{d^2\psi}{dr^2} \left( \frac{dr}{d\tilde{r}} \right)^2 \right]. \quad (3.19)$$

Corresponding to Eqs. 3.13 and 3.14, the Gaussian optical curvature can ultimately be expressed in the following precise form,

$$\mathcal{K} = -\Lambda m_0 e^{-2\gamma} + 3\Lambda q^2 e^{-\gamma} - 2\Lambda q^2 e^{-\gamma} \ln\left(\frac{r}{r_0}\right) - \frac{m_0 q^2 e^{-\gamma}}{r^2} + \mathcal{O}(m_0^2, \Lambda^2, q^4). \quad (3.20)$$

The obtained expression for Gaussian curvature indicates that it is influenced by various parameters, including mass, charge, MoaMax, cosmological constant, and length parameter.

## 4 Deflection of Light

In this section, we compute the deflection angle of a ModMax BTZ BH using the Gauss-Bonnet theorem (GBT). The GBT provides a connection between the intrinsic differential geometry of a metric associated with its topology within a regular domain is expressed as [42],

$$\iint_{U_R} \mathcal{K} dS + \oint_{\partial U_R} \kappa ds + \sum_z \beta_z = 2\pi\chi(U_R), \quad (4.1)$$

where  $U_R \subset \Sigma$  is a regular domain of a two-dimensional surface.  $\kappa$  denotes the geodesic curvature, defined as  $\kappa = \bar{g}(\nabla_{\dot{\sigma}}\dot{\sigma}, \ddot{\sigma})$ , where  $\sigma$  is a smooth curve of unit speed such that  $\bar{g}(\dot{\sigma}, \dot{\sigma}) = 1$ , and  $\ddot{\sigma}$  is the unit acceleration vector.  $\beta_z$  represents the exterior angle at the  $z$ -th vertex, and  $\chi$  is the Euler characteristic number. In the respective limit  $R \rightarrow \infty$  (for the curve  $C_R$ ), the geodesic curvature simplifies to  $\kappa(C_R) = |\nabla_{\dot{C}_R} \dot{C}_R|$ . The radial component of the geodesic curvature can be expressed as,

$$\left(\nabla_{\dot{C}_R} \dot{C}_R\right)^r = \dot{C}_R^\phi \partial_\phi \dot{C}_R^r + \Gamma_{\phi\phi}^r \left(\dot{C}_R^\theta\right)^2. \quad (4.2)$$

For sufficiently large  $R$ , the curve  $C_R$  is defined by  $r(\phi) = R = \text{constant}$ , leads to,

$$\left(\dot{C}_R^\phi\right)^2 = \frac{1}{\Psi^2(\bar{r})}. \quad (4.3)$$

In the context of optical geometry, the geodesic curvature can be expressed using the Christoffel symbols as,

$$\left(\nabla_{\dot{C}_R} \dot{C}_R\right)^r \rightarrow \frac{1}{R}. \quad (4.4)$$

This implies that  $\kappa(C_R) \rightarrow \frac{1}{R}$ . Using the optical metric defined in 3.12, we find  $dt = R d\phi$ . Consequently,

$$\kappa(C_R)dt = \lim_{R \rightarrow \infty} [\kappa(C_R)dt] = \lim_{R \rightarrow \infty} \left[ \frac{1}{2\sqrt{\bar{g}_{rr}\bar{g}_{\phi\phi}} \left(\frac{\partial \bar{g}_{\phi\phi}}{\partial r}\right)} \right] d\phi = d\phi. \quad (4.5)$$

Considering all these discussions, the Gauss-Bonnet theorem can be expressed as,

$$\iint_{U_R} \mathcal{K} dS + \oint_{\partial U_R} \kappa dt \Big|_{R \rightarrow \infty} = \iint_{S_\infty} \mathcal{K} dS + \int_{\pi+\delta}^0 d\phi. \quad (4.6)$$

In the weak deflection regime, the light ray at zeroth order follows a straight trajectory given by  $r(\phi) = \frac{b}{\sin\phi}$ , where  $b$  denotes the impact parameter. From this, the deflection angle can be derived as,

$$\tilde{\delta} = - \int_0^\pi \int_{b/\sin\phi}^\infty \mathcal{K} dS = - \int_0^\pi \int_{b/\sin\phi}^\infty \mathcal{K} \sqrt{\det \bar{g}} d\tilde{r} d\phi = - \int_0^\pi \int_{b/\sin\phi}^\infty \frac{\mathcal{K} r}{\psi(r)^{3/2}} d\tilde{r} d\phi. \quad (4.7)$$

Therefore, the deflection angle can be express as follows,

$$\tilde{\delta} = \frac{(m_0 e^{-\gamma} - 3q^2) e^{-\gamma}}{b\sqrt{\Lambda}} + \frac{2q^2 e^{-\gamma}}{b\sqrt{\Lambda}} (2 \ln(b) + \pi \ln(2) - 2[1 + \ln(r_0)]) - \frac{8m_0 q^2 e^{-\gamma}}{9b^2 \Lambda \sqrt{\Lambda}} + \mathcal{O}(m_0^2, \Lambda^2, q^4). \quad (4.8)$$

The deflection angle obtained in Eq. 4.8 demonstrates that it is directly proportional to the ModMax parameter and inversely proportional to the cosmological constant. When the ModMax parameter is set to zero, the deflection angle expression reduces to that of the charged BTZ BH, aligning with the findings of Upadhyay et al [48].

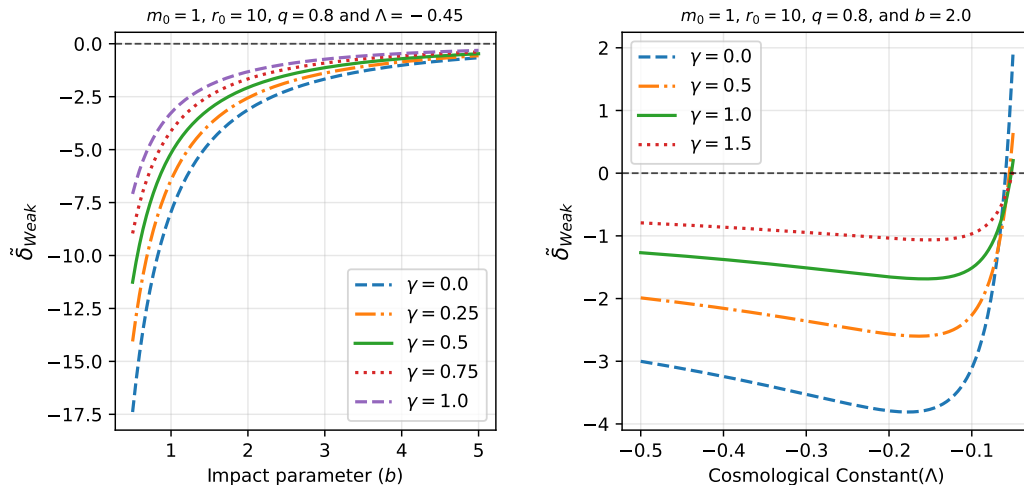


**Figure 6.** The variation of deflection angle with impact parameter (left panel) and cosmological constant (right panel) for different values of  $\gamma$ .

We analyze the behavior of the deflection angle as a function of the impact parameter and other BH parameters in detail. The graphical representations of these analyses are shown in Figs. 6 to 9. For large values of the charge parameter, the deflection angle increases with the impact parameter, highlighting the interplay between gravitational attraction and the repulsive effects introduced by the charge. Conversely, for decreasing values of the cosmological constant  $\Lambda$ , the deflection angle decreases, indicating a reduction in the curvature of spacetime in lower- $\Lambda$  environments. When examining the influence of the ModMax parameter, we observe a nuanced behavior. For the lowest values of the charge parameter, the deflection angle decreases with increasing ModMax parameter. In contrast, for higher values of the charge parameter, the deflection angle increases. This suggests that the combined effects of charge and ModMax parameter are interdependent, with the charge playing a dominant role in determining the net deflection behavior. Interestingly, beyond a specific critical value of the charge parameter, the deflection angle shifts to the negative region. This shift can be attributed to the additional repulsive force arising from the strong electromagnetic contribution in highly charged BHs. To explore this phenomenon further, we analyzed the deflection angle for lower charge parameter values. For these cases, the deflection angle decreases with the impact parameter for varying  $\gamma$  and  $\Lambda$ . Notably, higher values of  $\gamma$  correspond to lower deflection angles, indicating a reduction in the gravitational pull of the BH due to the increasing influence of the ModMax parameter. Additionally, larger values of the cosmological constant  $\Lambda$  result in greater deflection, consistent with the enhanced spacetime curvature. Finally, we compare our results with other BH solutions, specifically static BTZ BHs as shown in Fig. 9, under two scenarios as follows; **Case I: Low charge and low ModMax parameter:** In this case, the static BTZ BH exhibits the largest deflection angle, while the ModMax BTZ BH produces the smallest deflection. **Case II: High charge and**

**high ModMax parameter:** For this configuration, both charged and ModMax BTZ BHs exhibit negative deflection angles, reflecting the dominance of repulsive effects. However, the ModMax BTZ BH displays a larger deflection than the charged BTZ BH, signifying a more complex interaction between the ModMax parameter and the charge in determining the photon trajectories.

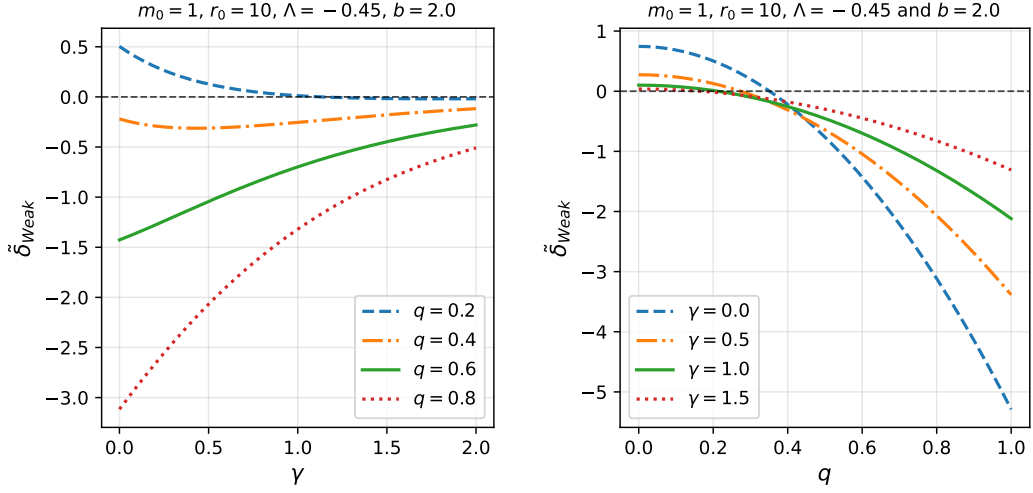


**Figure 7.** The variation of deflection angle with ModMax parameter (left panel) and charge parameter (right panel) including the different values of these parameters.

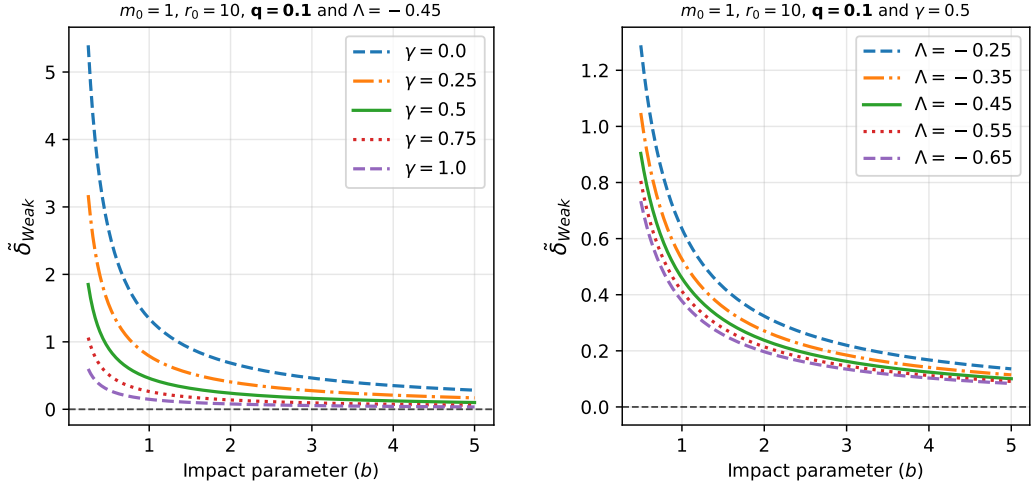


**Figure 8.** The variation of deflection angle with impact parameter for different values of  $\gamma$  (left panel) and  $\Lambda$  (right panel) for low value of charge parameter.

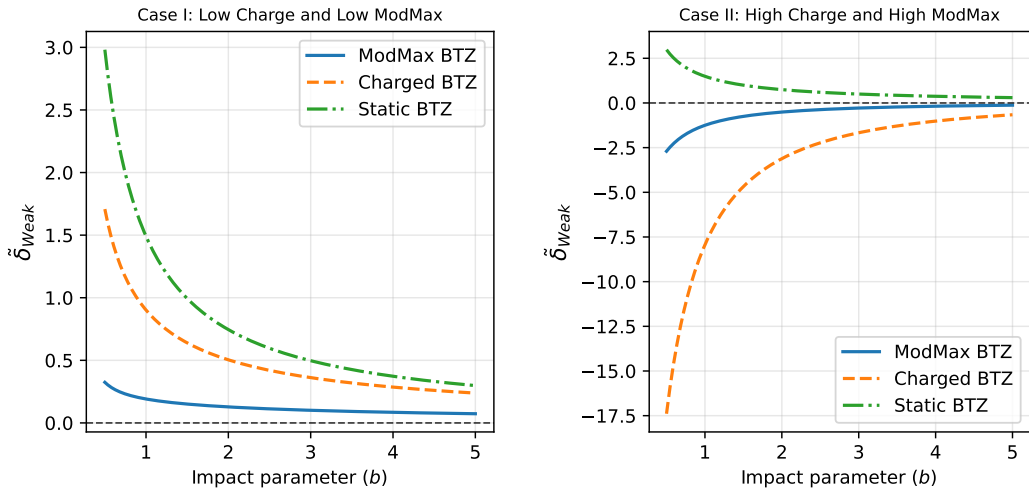


**Figure 9.** The variation of deflection angle with impact parameter and comparison of other BTZ BH solution. For Case I we consider  $\gamma = 0.5$  and  $q = 0.2$  and for Case II,  $\gamma = 1.5$  and  $q = 0.8$ .

## 5 Summary and conclusions

In this work, we study the propagation of massless particles around the ModMax BTZ BH. We examine the horizon structure, null geodesics, possible types of photon trajectories, and the stability of null geodesics. Thereafter, we have computed the deflection angle using the Gauss-Bonnet theorem. The main findings of the study can be summarized below:

- **Horizon Structure:** We analyzed the behavior of the metric function with respect to the radial distance to investigate the nature of the horizons. It was observed that small charged AdS BTZ BH with large values of the ModMax parameter exhibit two distinct roots: the inner horizon and the event horizon. Notably, the BH horizons are independent of the cosmological constant.
- **Photon Motion:** We obtained the null geodesics using the Lagrangian approach. The graphical representation of the effective potential indicates that unstable photon orbits are not possible, although marginally stable circular orbits may exist. Photon sphere radius analysis, reveal that it decreases with increasing  $\gamma$  while, increases with increasing  $q$ . The possible trajectories, determined by the angular momentum and energy of massless particles as well as the BH parameters, include both bound orbits and flyby trajectories.
- **Stability of Null Geodesics:** We examine the stability of null geodesics using a dynamical system approach. The values of  $\gamma$  and  $q$  have been observed to increase the influence of the BH parameters, altering the stability and behavior of the photon orbit.
- **Deflection Angle Behavior:** The deflection angle increases with the impact parameter for large charge values but decreases with a smaller cosmological constant. Furthermore, a higher  $\gamma$  value reduces the gravitational pull, leading to lower deflection angles.

- **ModMax Parameter Effect:** For low charge values, the deflection angle decreases with increasing ModMax parameter. In contrast, at higher charge values, the deflection angle increases, demonstrating an interaction between the charge and the ModMax parameter. Beyond a critical charge parameter, the deflection angle shifts to the negative region because of repulsive forces from the electromagnetic field, particularly in highly charged BH.
- **Comparison with Static and Charged BTZ BHs:** The static BTZ BH exhibits a greater deflection for a lower charge and a lower ModMax parameter. For higher charges and higher ModMax values, both the charged and the ModMax BTZ BH show negative deflection, with the ModMax BTZ BH exhibiting a larger magnitude. Physically, this indicates that in the presence of a significant charge and ModMax parameter, this particular BH solution predominantly emphasizes the dominance of repulsive interactions experienced by massless particles.

The obtained results will be crucial for understanding the behavior of light propagation in the context of modified nonlinear dynamics around lower-dimensional BHs. However, constraining the theoretical results obtained with the observational data from the EHT collaboration remains a challenge. Nevertheless, by comparing theoretical models of astrophysical BHs with observational results, we can explore how they differ from lower-dimensional BHs, providing valuable insights for future studies.

## Acknowledgements

The author sincerely acknowledges IMSc for providing excellent facilities and a conducive environment to carry out his research as a postdoctoral fellow at the Institute. The author is very thankful to Prof. Hemwati Nandan from the Department of Physics, Hemwati Nandan Bahuguna Garhwal University, Srinagar, Uttarakhand, India, for his kind support and help during this research.

## References

- [1] W. Heisenberg and H. Euler, *Consequences of Dirac's theory of positrons*, *Z. Phys.* **98** (1936) 714 [[physics/0605038](#)].
- [2] J. Schwinger, *On gauge invariance and vacuum polarization*, *Physical Review* **82** (1951) 664.
- [3] H. Yajima and T. Tamaki, *Black hole solutions in Euler-Heisenberg theory*, *Phys. Rev. D* **63** (2001) 064007 [[gr-qc/0005016](#)].
- [4] C. Baccigalupi, F. Perrotta, G. De Zotti, G.F. Smoot, C. Burigana, D. Maino et al., *Extracting cosmic microwave background polarisation from satellite astrophysical maps*, *Mon. Not. Roy. Astron. Soc.* **354** (2004) 55 [[astro-ph/0209591](#)].
- [5] E. Ayon-Beato and A. Garcia, *Nonsingular charged black hole solution for nonlinear source*, *Gen. Rel. Grav.* **31** (1999) 629 [[gr-qc/9911084](#)].
- [6] V.A. De Lorenci, R. Klippert, M. Novello and J.M. Salim, *Nonlinear electrodynamics and FRW cosmology*, *Phys. Rev. D* **65** (2002) 063501.
- [7] I. Dymnikova, *Regular electrically charged structures in nonlinear electrodynamics coupled to general relativity*, *Class. Quant. Grav.* **21** (2004) 4417 [[gr-qc/0407072](#)].
- [8] C. Corda and H.J. Mosquera Cuesta, *Removing black-hole singularities with nonlinear electrodynamics*, *Mod. Phys. Lett. A* **25** (2010) 2423 [[0905.3298](#)].

- [9] M. Born and L. Infeld, *Foundations of the new field theory*, *Proc. Roy. Soc. Lond. A* **144** (1934) 425.
- [10] M. Hassaine and C. Martinez, *Higher-dimensional black holes with a conformally invariant Maxwell source*, *Phys. Rev. D* **75** (2007) 027502 [[hep-th/0701058](#)].
- [11] H. Maeda, M. Hassaine and C. Martinez, *Lovelock black holes with a nonlinear Maxwell field*, *Phys. Rev. D* **79** (2009) 044012 [[0812.2038](#)].
- [12] I. Bandos, K. Lechner, D. Sorokin and P.K. Townsend, *Nonlinear duality-invariant conformal extension of maxwell's equations*, *Physical Review D* **102** (2020) 121703.
- [13] B. Kosyakov, *Nonlinear electrodynamics with the maximum allowable symmetries*, *Physics Letters B* **810** (2020) 135840.
- [14] S.I. Kruglov, *On generalized ModMax model of nonlinear electrodynamics*, *Phys. Lett. B* **822** (2021) 136633 [[2108.08250](#)].
- [15] S.M. Kuzenko and E.S.N. Raptakis, *Duality-invariant superconformal higher-spin models*, *Phys. Rev. D* **104** (2021) 125003 [[2107.02001](#)].
- [16] Z. Avetisyan, O. Evnin and K. Mkrtchyan, *Democratic Lagrangians for Nonlinear Electrodynamics*, *Phys. Rev. Lett.* **127** (2021) 271601 [[2108.01103](#)].
- [17] M. Banados, C. Teitelboim and J. Zanelli, *The Black hole in three-dimensional space-time*, *Phys. Rev. Lett.* **69** (1992) 1849 [[hep-th/9204099](#)].
- [18] M. Banados, M. Henneaux, C. Teitelboim and J. Zanelli, *Geometry of the (2+1) black hole*, *Phys. Rev. D* **48** (1993) 1506 [[gr-qc/9302012](#)].
- [19] H. Quevedo and A. Sanchez, *Geometric description of BTZ black holes thermodynamics*, *Phys. Rev. D* **79** (2009) 024012 [[0811.2524](#)].
- [20] M. Cardenas, O. Fuentealba and C. Martínez, *Three-dimensional black holes with conformally coupled scalar and gauge fields*, *Phys. Rev. D* **90** (2014) 124072 [[1408.1401](#)].
- [21] S. Hossein Hendi, B. Eslam Panah, S. Panahiyan and M. Hassaine, *BTZ dilatonic black holes coupled to Maxwell and Born-Infeld electrodynamics*, *Phys. Rev. D* **98** (2018) 084006 [[1712.04328](#)].
- [22] G.G.L. Nashed and S. Capozziello, *Charged Anti-de Sitter BTZ black holes in Maxwell-f(T) gravity*, *Int. J. Mod. Phys. A* **33** (2018) 1850076 [[1710.06620](#)].
- [23] B. Mu, J. Tao and P. Wang, *Free-fall Rainbow BTZ Black Hole*, *Phys. Lett. B* **800** (2020) 135098 [[1906.11703](#)].
- [24] P. Cañate, D. Magos and N. Breton, *Nonlinear electrodynamics generalization of the rotating BTZ black hole*, *Phys. Rev. D* **101** (2020) 064010 [[2002.00890](#)].
- [25] B. Eslam Panah, *Charged Accelerating BTZ Black Holes*, *Fortsch. Phys.* **71** (2023) 2300012 [[2203.12619](#)].
- [26] T. Karakasis, G. Koutsoumbas and E. Papantonopoulos, *Black holes with scalar hair in three dimensions*, *Phys. Rev. D* **107** (2023) 124047 [[2305.00686](#)].
- [27] B. Eslam Panah, M. Khorasani and J. Sedaghat, *Three-dimensional accelerating AdS black holes in F(R) gravity*, *Eur. Phys. J. Plus* **138** (2023) 728 [[2309.02472](#)].
- [28] B. Eslam Panah, *Thermodynamics and thermal stability of btz-modmax black holes*, *Contributions of Science and Technology for Engineering* **1** (2024) 25.
- [29] C.W. Misner, K.S. Thorne and J.A. Wheeler, *Gravitation*, W. H. Freeman, San Francisco (1973).
- [30] N. Cruz, C. Martinez and L. Pena, *Geodesic structure of the (2+1) black hole*, *Class. Quant. Grav.* **11** (1994) 2731 [[gr-qc/9401025](#)].



- [31] A. Dasgupta, H. Nandan and S. Kar, *Geodesic flows in rotating black hole backgrounds*, *Phys. Rev. D* **85** (2012) 104037 [[1202.5370](#)].
- [32] F. Rahaman, P.K.F. Kuhfittig, B.C. Bhui, M. Rahaman, S. Ray and U.F. Mondal, *BTZ black holes inspired by noncommutative geometry*, *Phys. Rev. D* **87** (2013) 084014 [[1301.4217](#)].
- [33] W. Xu and D.-C. Zou, *(2 + 1) -Dimensional charged black holes with scalar hair in Einstein–Power–Maxwell Theory*, *Gen. Rel. Grav.* **49** (2017) 73 [[1408.1998](#)].
- [34] S. Soroushfar, R. Saffari and A. Jafari, *Study of geodesic motion in a ( 2+1 )-dimensional charged BTZ black hole*, *Phys. Rev. D* **93** (2016) 104037 [[1512.08449](#)].
- [35] S.H. Hendi, A.M. Tavakkoli, S. Panahiyan, B. Eslam Panah and E. Hackmann, *Simulation of geodesic trajectory of charged BTZ black holes in massive gravity*, *Eur. Phys. J. C* **80** (2020) 524 [[2002.01302](#)].
- [36] S. Kala, H. Nandan, P. Sharma and M. Elmardi, *Geodesics and bending of light around a BTZ black hole surrounded by quintessential matter*, *Mod. Phys. Lett. A* **36** (2021) 2150224 [[2109.14991](#)].
- [37] S.L. Jaki, *Johann georg von soldner and the gravitational bending of light, with an english translation of his essay on it published in 1801*, *Foundations of Physics* **8** (1978) 927.
- [38] C.G. Darwin, *The gravity field of a particle*, *Proceedings of the Royal Society of London. Series A. Mathematical and Physical Sciences* **249** (1959) 180.
- [39] K.S. Virbhadra and G.F.R. Ellis, *Schwarzschild black hole lensing*, *Phys. Rev. D* **62** (2000) 084003 [[astro-ph/9904193](#)].
- [40] S.V. Iyer and A.O. Petters, *Light’s bending angle due to black holes: From the photon sphere to infinity*, *Gen. Rel. Grav.* **39** (2007) 1563 [[gr-qc/0611086](#)].
- [41] W. Rindler and M. Ishak, *Contribution of the cosmological constant to the relativistic bending of light revisited*, *Phys. Rev. D* **76** (2007) 043006 [[0709.2948](#)].
- [42] G.W. Gibbons and M.C. Werner, *Applications of the Gauss-Bonnet theorem to gravitational lensing*, *Class. Quant. Grav.* **25** (2008) 235009 [[0807.0854](#)].
- [43] V. Bozza, *Gravitational Lensing by Black Holes*, *Gen. Rel. Grav.* **42** (2010) 2269 [[0911.2187](#)].
- [44] A. Ishihara, Y. Suzuki, T. Ono, T. Kitamura and H. Asada, *Gravitational bending angle of light for finite distance and the Gauss-Bonnet theorem*, *Phys. Rev. D* **94** (2016) 084015 [[1604.08308](#)].
- [45] T. Ono and H. Asada, *The effects of finite distance on the gravitational deflection angle of light*, *Universe* **5** (2019) 218 [[1906.02414](#)].
- [46] M. Fathi, A. Rincón and J.R. Villanueva, *Photon trajectories on a first order scale-dependent static BTZ black hole*, *Class. Quant. Grav.* **37** (2020) 075004 [[1903.09037](#)].
- [47] S. Kala, H. Nandan and P. Sharma, *Deflection of Light Around a Rotating BTZ Black Hole*, *Mod. Phys. Lett. A* **35** (2020) 2050323 [[2010.16183](#)].
- [48] S. Upadhyay, S. Mandal, Y. Myrzakulov and K. Myrzakulov, *Weak deflection angle, greybody bound and shadow for charged massive BTZ black hole*, *Annals Phys.* **450** (2023) 169242 [[2303.02132](#)].
- [49] E. Guzman-Herrera and N. Breton, *Light propagation in the vicinity of the ModMax black hole*, *JCAP* **01** (2024) 041 [[2308.12572](#)].
- [50] K. Nakashi, S. Kobayashi, S. Ueda and H. Saida, *Null Geodesics and Repulsive Behavior of Gravity in (2+1)-dimensional Massive Gravity*, *PTEP* **2019** (2019) 073E02 [[1901.06098](#)].

- [51] P.A. González, M. Olivares, E. Papantonopoulos and Y. Vásquez, *Motion and trajectories of photons in a three-dimensional rotating Hořava-AdS black hole*, *Phys. Rev. D* **101** (2020) 044018 [[1912.00946](#)].
- [52] B. Narzilloev, S. Shaymatov, I. Hussain, A. Abdujabbarov, B. Ahmedov and C. Bambi, *Motion of Particles and Gravitational Lensing Around (2+1)-dimensional BTZ black holes in Gauss-Bonnet Gravity*, *Eur. Phys. J. C* **81** (2021) 849 [[2109.02816](#)].
- [53] M.D. Sultan, S. Chaudhary, A. Malik and M.M. Alam, *Optical aspects of Born-Infeld BTZ black holes in massive gravity*, *Phys. Scripta* **99** (2024) 125014.
- [54] S.H. Hendi, *Charged BTZ-like Black Holes in Higher Dimensions*, *Eur. Phys. J. C* **71** (2011) 1551 [[1007.2704](#)].
- [55] R.M. Corless, G.H. Gonnet, D.E. Hare, D.J. Jeffrey and D.E. Knuth, *On the lambert w function*, *Advances in Computational mathematics* **5** (1996) 329.
- [56] E. Hackmann, *Geodesic equations in black hole space-times with cosmological constant*, Ph.D. thesis, Bremen U., 2010.
- [57] I. Goldhirsch, P.-L. Sulem and S.A. Orszag, *Stability and lyapunov stability of dynamical systems: A differential approach and a numerical method*, *Physica D: Nonlinear Phenomena* **27** (1987) 311.
- [58] S. Yang, J. Tao, B. Mu and A. He, *Lyapunov exponents and phase transitions of Born-Infeld AdS black holes*, *JCAP* **07** (2023) 045 [[2304.01877](#)].